Sensing and Bio-Sensing Research 33 (2021) 100445

Contents lists available at ScienceDirect

Sensing and Bio-Sensing Research

journal homepage: www.elsevier.com/locate/sbsr

Electrochemical immunosensor for detection of CA 15-3 biomarker in point-of-care

Tânia S.C.R. Rebelo [a,b], José A. Ribeiro [a,*], M. Goreti F. Sales [b,c], Carlos M. Pereira [a,*]

[a] CIQUP, Department of Chemistry and Biochemistry, Faculty of Sciences of University of Porto, Rua do Campo Alegre 687, s/n, Porto 4169-007, Portugal
[b] BioMark/UC, Department of Chemical Engineering, Faculty of Sciences and Technology, Coimbra University, Rua Silvio Lima, 3030-790 Coimbra, Portugal
[c] CEB, Centre of Biological Engineering, Minho University, Campus de Gualtar, 4710-057 Braga, Portugal

ARTICLE INFO

Keywords:
CA 15-3
Cancer biomarker
Electrochemical biosensor
Immunosensor
Screen-printed electrode (SPE)
Point-of-care (PoC) analysis

ABSTRACT

This work reports the development of a simple and rapid electrochemical immunosensor for the determination of breast cancer biomarker Cancer Antigen 15–3 (CA 15–3). Disposable and cost-effective chips, consisting of gold screen-printed electrodes (AuSPEs), were used to develop the portable electrochemical devices for monitoring the biomarker in point-of-care (PoC), under clinical context.

The biosensor preparation consisted of two simple steps. First, a self-assembled monolayer (SAM) of mercaptosuccinic acid (MSA) was formed at the AuSPE surface. Then, the CA 15–3 antibody was covalently bound to the carboxylic groups standing at the electrode surface using EDC/NHS chemistry.

The performance of the developed immunosensor was evaluated by assessing the sensor sensitivity, linear response interval, selectivity and detection limit (LOD). The developed immunosensor provided a wide linear concentration range (from 1.0 to 1000 U mL^{-1}) and low detection levels were achieved (LOD of 0.95 U mL^{-1}), enabling the sensitive detection of the cancer biomarker at clinically relevant levels, using square wave voltammetry (SWV) as electroanalytical technique. Moreover, selectivity studies performed against other cancer biomarkers (CA 125 and CA 19–9) revealed that the antibody has high selectivity for CA 15–3 antigen. The immunosensor was applied to the quantification of CA 15–3 in artificial serum samples with satisfactory results.

1. Introduction

In 2018, cancer was responsible for 9.6 million deaths, being the second leading cause of death in the world. Among all cancer diseases, breast cancer is the third most common cancer, with an incidence level of 11.6% and a mortality rate of 6.6%, thus, affecting millions of women worldwide [1].

Cancer biomarkers play an important role in disease screening and treatment follow-up. The Carbohydrate Antigen 15-3 (CA 15–3) antigen, a member of the mucin-1 (MUC-1) family of glycoproteins, is the most widely used serum marker for breast cancer, being used in the detection of metastases and follow-up of the women with breast cancer [2,3]. The normal level of this biomarker in the serum is lower than 30 U mL^{-1} but, if the total CA 15-3 level serum significantly increases, this may be indicative of breast cancer disease [3,4]. Therefore, simple, sensitive and reliable methodologies for CA 15-3 detection are currently required for the early disease diagnosis and patient response to treatment.

Most common methods for determining CA 15–3 biomarker rely on immunoassays, manly through ELISA tests [5,6]. Meanwhile, other immunoassays emerged on the literature, differing only in the approach signal transduction, such as chemiluminescence [7,8], electrochemiluminescence [9,10], fluorescence [11,12], surface-enhanced raman spectroscopy (SERS) [13] and electrochemical readout [14–20]. However, these immunosensor usually requires labels and/or secondary antibodies for signal amplification, making detection procedures complicated, time-consuming, very dependent on laboratory instrumentation and rather expensive. Thus, the development of novel simple, fast and cost-effective devices for sensitive detection of CA 15–3 biomarker, suitable for point-of-care (PoC) analysis, is currently a demand.

In this work, we suggest a novel cheap and disposable electrochemical immunosensor, having simple and rapid construction, that can quickly detect the target biomarker in PoC. Disposable and cost-effective chips, consisting of gold screen-printed electrodes (AuSPEs), were used to develop the portable electrochemical devices. Electrochemical signals of specific antibody-antigen interaction were easily transduced by

* Corresponding authors.
E-mail addresses: jose.ribeiro@fc.up.pt (J.A. Ribeiro), cmpereir@fc.up.pt (C.M. Pereira).

https://doi.org/10.1016/j.sbsr.2021.100445
Received 26 May 2021; Received in revised form 26 July 2021; Accepted 28 July 2021
Available online 30 July 2021

performing electrochemical measurements in the presence of biocompatible ferrocyanide/ferricyanide redox probe as reporting system. The basic features of the proposed immunosensor are illustrated in Scheme 1.

To build the sensor platforms, a self-assembled monolayer (SAM) of mercaptosuccinic acid (MSA) was initially deposited on the surface of a AuSPE to form a narrow carboxylic-acid-terminated monolayer [21,22]. Then, the CA 15–3 antibody was coupled to the carboxylic groups standing at the electrode surface through NHS/EDC method [23,24] (see Scheme 2). In order to evaluate the performance of the electrochemical immunosensor, a systematic investigation of several analytical parameters (such as sensitivity, dynamic linear range, LOD and selectivity) was performed in buffer solution. After that, the developed immunosensor was applied for the determination of the CA 15–3 biomarker in artificial serum samples.

2. Material and methods

2.1. Apparatus

The electrochemical data were recorded with a computer-controlled potentiostat Autolab PGSTAT20 (Eco Chemie, Netherlands), controlled by the NOVA 2.4.1 software. Gold screen-printed electrodes (AuSPEs, 4 mm diameter, DRP-220AT, DropSens, Merck) were used as sensor platforms. The AuSPEs were connected to the potentiostat by means of a suitable box, also bought from DropSens (Merck). All experiments were carried out at room temperature.

The SPR experiments were conducted using a SPR Autolab ESPRIT (KEI bv, The Netherlands) controlled by KEI SPR Data Acquisition software (version 4.4). Prior to the SPR experiments, the flat glass disks coated with a thin gold film (≈50 nm, KEI bv, the Netherlands) were washed thoroughly with pure water and ethanol, followed by drying under N_2 flow. The SPR gold disks were then placed over the half-cylinder glass prism covered with a thin layer of refractive-index-matching oil and stand positioned inside the equipment in a Kretschmann optical configuration to begin the measurements of the SPR reflected angle (in milidegrees, m°). The temperature of the SPR cell was maintained constant and reproducible by using a Julabo F32-HE (Germany) water bath. All experiments were carried out at 25.0 °C.

2.2. Reagents and solutions

MUC-1 antigen (10.9 kU mL^{-1}, American Research Products), anti-mucin 1 rabbit polyclonal antibody (anti-CA 15–3, St John's Laboratory), potassium ferricyanide ($K_3[Fe(CN)_6]$, Merck), potassium ferrocyanide trihydrate ($K_4[Fe(CN)_6]$, Merck), sodium chloride (Panreac), sodium hydrogen carbonate (Merck), bovine serum albumin (BSA, ≥98%, Sigma-Aldrich), mercaptosuccinic acid (MSA, ≥98%, Merck), N-(3-dimethylaminopropyl)-N′-ethylcarbodiimide (EDC, 98 + %, Alfa Aesar), N-hydroxysuccinimide (NHS, 98%, Aldrich), ethanolamine (EA, ≥98%, Sigma-Aldrich), sodium sulfate (Na_2SO_4, Sigma-Aldrich), sodium dihydrogen phosphate (Sigma-Aldrich), sodium hydrogen phosphate (Sigma-Aldrich), sodium acetate (Sigma-Aldrich), acetic acid (Sigma-Aldrich) were used as received.

Water purified with a Milli-Q purification system (Millipore, resistivity >18 MΩ cm) was used for cleaning and solutions preparation.

Standard stock solutions of CA 15–3 (5.2×10^3 U mL^{-1}) were prepared in 10 mmol L^{-1} acetate buffer solution (pH 4.0) and stored at −20 °C if not in use. Less concentrated standards were prepared by suitable dilutions of this solution, in the same buffer.

Artificial serum solution used had the following composition: 7.01 g L^{-1} NaCl, 1.68 g L^{-1} $NaHCO_3$ and 30 g L^{-1} BSA (pH 7.3) [25].

2.3. Fabrication of immunosensor

The AuSPE was first cleaned with pure water, acetone and ethanol. Then, the chip was electrochemically cleaned in a 0.5 mol L^{-1} sulfuric acid solution using cyclic voltammetry (CV), applied between 0 and 1.25 V, with a 0.1 V s^{-1} scan rate, until the voltammogram becomes stable (approximately 12 cycles). Then, the AuSPE was thoroughly rinsed with pure water and dried under a nitrogen stream.

To sensor platforms were prepared by simple immobilization of bioreceptors over a pre-formed SAM using EDC/NHS chemistry (see Scheme 2). Firstly, the working area of the AuSPE was incubated with a 10 mmol L^{-1} MSA aqueous solution overnight to build the SAM due to the strong interaction between the thiol group (-SH) and the gold surface [21,22]. After the SAM formation, the AuSPE was rinsed with pure water and then dried under a nitrogen stream. Then, the working area of the AuSPE was incubated with a 10 mmol L^{-1} equimolar mixture of NHS and EDC [23,24] for 30 min, followed by rinsing with PBS and surface drying. After that, the electrode working area was incubated with a solution of CA 15–3 antibody (prepared in 10 mmol L^{-1} acetate buffer, pH 4.0) for 90 min, at 4 °C. After antibody immobilization, the chip surface was rinsed with acetate buffer, followed by surface drying. Finally, the remaining reactive sites were blocked by incubating the sensor surface with a 10 mmol L^{-1} ethanolamine solution (pH 8.0) for

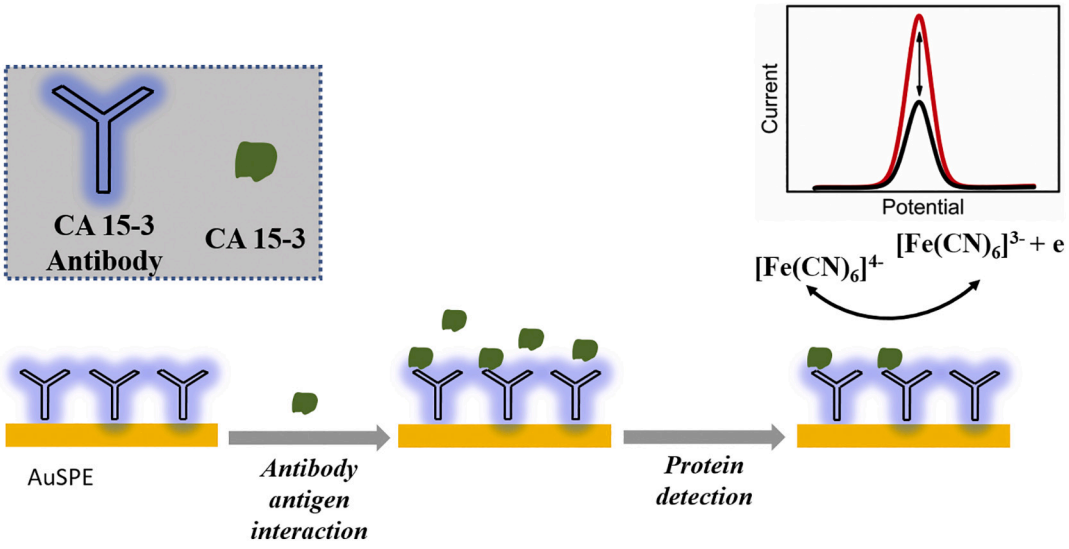

Scheme 1. Schematic representation showing the different steps involved in the electrochemical detection of CA 15–3 biomarker.

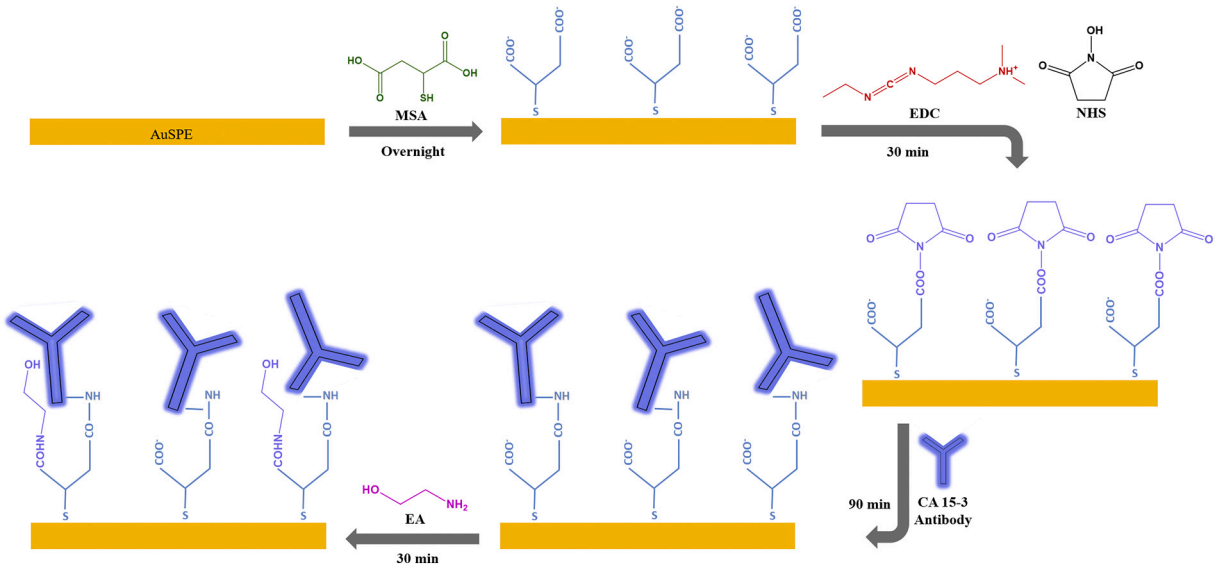

Scheme 2. Schematic representation of the procedure for CA 15–3 antibody immobilization on the AuSPE surface.

30 min. After surface washing and drying, the resulting modified chip was stored at 4 °C until use.

2.4. Electrochemical measurements

The electrochemical measurements were carried out in a 5 mmol L^{-1} equimolar solution of $[Fe(CN)_6]^{3-}$ and $[Fe(CN)_6]^{4-}$, dissolved in 0.1 mol L^{-1} Na_2SO_4 as electrolyte solution. Preliminary experiments revealed that higher peak currents were achieved in Na_2SO_4 relatively to PBS (see Fig. S1, SI). In SWV measurements, the potential was scanned from −0.30 to 0.40 V, at a frequency of 10 Hz, with an amplitude of 50 mV and a step potential of 2 mV.

2.5. Calibration curves and determination of CA 15-3 in artificial serum

Detection studies were performed by incubating the sensing platforms for 30 min with CA 15–3 standard solutions (ranging from 0.10 to 1000 U mL^{-1}, prepared in 10 mmol L^{-1} acetate buffer, pH 4.0), followed by electrochemical measurements in the presence of the selected redox probe couple. Calibration curves were built by plotting the redox probe peak current (I_{peak}) values obtained from the SWV measurements against the logarithmic of CA 15–3 concentration.

To perform the detection of CA 15–3 in artificial serum, serum samples were previously diluted 20 times in acetate buffer and then spiked with known amounts of CA 15–3 (from 0.30 to 400 U mL^{-1}). All assays were conducted in triplicate.

3. Results and discussion

3.1. Step-by-step fabrication of the immunosensor

In this work, the immunosensor stability and improved response relied on successful modification of the electrode surface concerning the immobilization of biorecognition element. Preliminary studies were performed for optimization of experimental conditions (association buffer composition, pH, antibody concentration, reaction times, etc.) for the effective antibody immobilization at the chip surface (see Fig. S2, SI). Two CA 15–3 antibody solutions (diluted to concentration levels of 50 and 20 μg mL^{-1}) in buffer solutions 10 mmol L^{-1} PBS pH 7.2 and 10 mmol L^{-1} acetate buffer pH 4.0 were tested. After performing the electrochemical experiments, an optimal CA 15–3 antibody concentration of 20 μg mL^{-1}, prepared in low ionic strength acidic buffer solution (10 mmol L^{-1} Na-acetate buffer, at pH 4.0) as association buffer, was selected for the immunosensor preparation. The results obtained suggested that some of the unreacted carboxylic acid groups, after EDC/NHS activation, remained negatively charged at the SAM surface (pKa values of MSA lie in the range 3–5 [26,27]) contributing to preconcentrate the positively charged amino acid residues in the CA 15–3 antibody. Furthermore, electrostatic attraction in low ionic strength medium was reported in the literature as key mechanism for immobilization of proteins on the biosensing surfaces [28–30]. By opposition, the use of the high ionic strength buffers does not benefit from electrostatic attraction of antibodies to the sensing surface since hydrophobic mechanisms dominates [31], thus, decreasing the amount of bioreceptors immobilized.

All surface modifications were followed by electrochemical measurements in the presence of $[Fe(CN)_6]^{3-/4-}$ redox probe solution, as shown in Fig. 1A. Furthermore, the estimated peak current (I_{peak}) values are resumed in Table S1 (SI). As can be seen in the figure, the peak current decreased after surface incubation with 10 mmol L^{-1} MSA solution, confirming the spontaneous formation of a carboxylic-acid-terminated monolayer over the sensor surface [22]. After SAM activation with a solution of NHS/EDC, the CA 15–3 antibody was immobilized on the AuSPE surface via covalent bond with the available unstable esters groups [24], causing an additional barrier to the diffusional redox probe, thus, decreasing the measured peak current. Finally, the remaining unreacted active sites were blocked by reaction with ethanolamine [24], leading to a further decrease o redox probe peak current.

Furthermore, the antibody immobilization procedure used in this work was also evaluated by SPR technique. During the SPR measurements, all buffers and solutions were automatically injected into the measuring channel while monitoring the angle changes occurring at the dielectric thin metal film [32,33]. The real-time step-by-step construction of the immunosensor on the SPR gold chips is shown in Fig. 1B. The sensorgram profile achieved confirms the electrochemical data collected about the successful immobilization of the CA 15–3 antibody at the gold substrates under the previously optimized experimental conditions. After the injection of the CA 15–3 antibody, the overall angle shift prior to the surface deactivation with ethanolamine (step 7) is of about 400 m°, which corresponds to an amount of antibody attached of ~3.3 ng mm^{-2} [34].

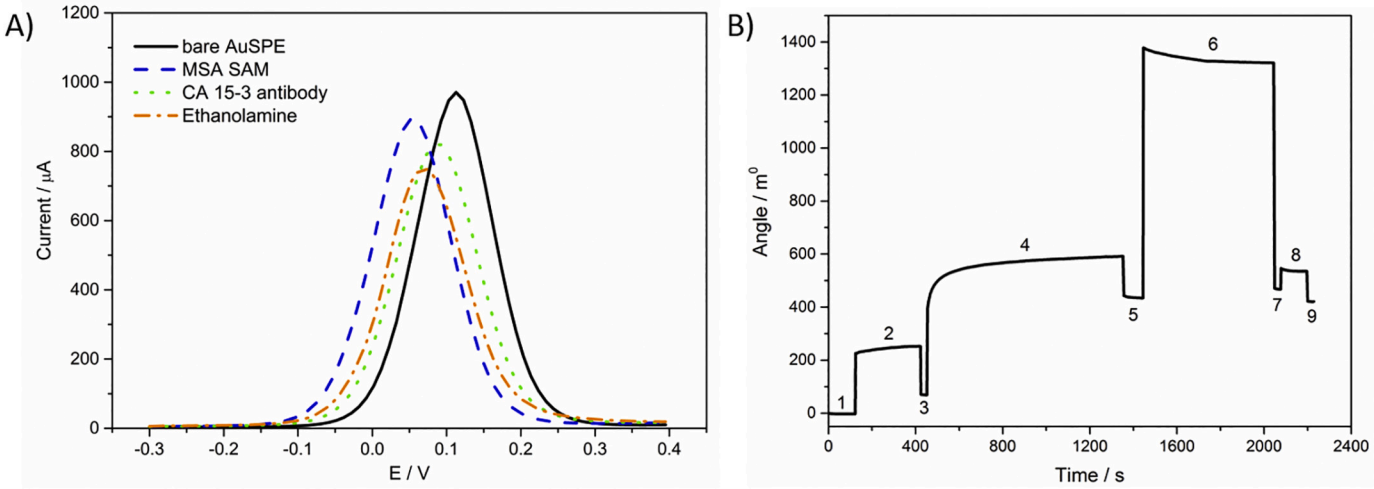

Fig. 1. A) SWV voltammograms, recorded in the presence of 5 mmol L^{-1} $[Fe(CN)_6]^{3-/4-}$, prepared in 0.1 mol L^{-1} Na_2SO_4 electrolyte solution, after each modification step occurring at the AuSPE surface. B) SPR sensor response to the immobilization of CA 15–3 antibody on the Au sensor surface, previously modified with MSA SAM. Step 1: injection of 10 mmol L^{-1} PBS, pH 7.4, for 120 s (baseline); Step 2: activation of MSA SAM with a mixture of EDC/NHS (50 mmol L^{-1}, in water) for 300 s; Step 3: wash with PBS for 30 s (baseline); Step 4: immobilization of CA 15–3 antibody (20 µg mL^{-1}, in 10 mmol L^{-1} acetate buffer solution, pH 4.0) for 900 s; Step 5: wash with PBS for 90 s (baseline); Step 6: deactivation of unreacted esters with ethanolamine (1 mol L^{-1}, pH 8.0) for 600 s; Step 7: wash with PBS for 30 s (baseline); Step 8: wash with PBS, containing 0.1% SDS, for 120 s; Step 9: wash with PBS for 30 s (baseline).

3.2. Optimization of the immunoreaction

For comprehensive understanding of antigen binding capacity for immobilized antibodies as function of medium pH, the analytical response of the developed immunosensor was evaluated at different pH values. The electrochemical signals, obtained from SWVs recorded (see Fig. S3, SI) after incubating the sensor surface with several CA 15–3 solutions (from 0.010 to 100 U mL^{-1}) prepared in buffer solution at pH 7.2 and at pH 4.0, are shown in Fig. 2. The decrease of the redox probe peak current was more pronounced for antigen solutions prepared at pH 4.0 relatively to physiological pH for the several concentrations of biomarker tested. Thus, more acid medium pH seems to improve the extension of the immunoreaction probably due to electrostatic attraction between positively charged protein (isoelectric point of CA 15–3 protein is predicted to be between 3 and 5 [35]) and the antibody binding sites, which are expected to be negatively charged. Therefore, 10 mmol L^{-1} acetate buffer at pH 4.0 was used to perform the immunosensing studies.

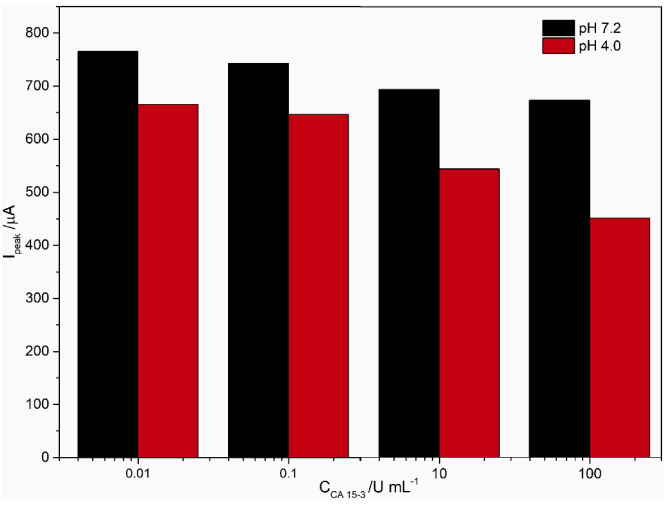

Fig. 2. Redox probe peak current obtained from the SWV measurements, performed in the presence of 5 mmol L^{-1} $[Fe(CN)_6]^{3-/4-}$, after surface incubation with different CA 15–3 solutions prepared in 10 mmol L^{-1} PBS pH 7.2 and 10 mmol L^{-1} acetate buffer pH 4.0. The concentrations of CA 15–3 tested ranged from 0.010 to 100 U mL^{-1}.

The formation of the immunocomplex between immobilized CA 15–3 antibody and the CA 15–3 antigen in solution was also studied in real-time by SPR. The sensorgrams collected for the various concentrations of CA 15–3 tested (from 1.0 to 500 U mL^{-1}), prepared in acetate buffer solution (pH 4.0), are depicted in Fig. 3. As can be seen in the figure, the SPR angle increased as the binding event occurs until dynamic equilibrium was reached. The SPR angle variation increased with the increasing concentration of CA 15–3. Similar studies were performed

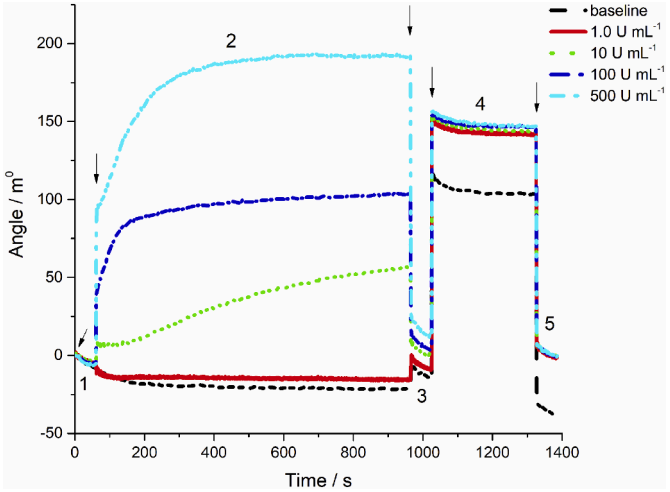

Fig. 3. Real-time SPR monitoring of the interaction between immobilized antibody on SPR gold substrates and CA 15–3 in solution. The concentrations of CA 15–3 tested ranged from 1.0 to 500 U mL^{-1}. Line 1: baseline collected in 10 mmol L^{-1} PBS, pH 7.4, for 60 s; Line 2: real-time monitoring of the antigen-antibody interaction for 15 min; Line 3: surface wash with 10 mmol L^{-1} PBS, pH 7.4, for 60 s (return to baseline); For comparison, the response obtained after injection of association buffer (10 mmol L^{-1} acetate buffer solution, pH 4.0, without CA 15–3) into the measuring channel (dashed line) is also shown in the figure; Line 4: surface regeneration after wash with glycine-HCl buffer solution (pH 2.0) for 300 s; Line 5: wash with 0.010 mol L^{-1} PBS, pH 7.4, for 60 s (return to baseline). (For interpretation of the references to colour in this figure legend, the reader is referred to the web version of this article.)

for CA 15–3 dissolved in PBS at pH 7.2, however, no appreciable angle change was observed, except for the higher concentration level of antigen (data not shown), meaning that antibody-antigen interaction is more favourable under more acidic conditions.

3.3. Analytical response of the electrochemical immunosensor

In order to study the analytical performance of the developed immunosensor, the AuSPE surface was incubated with solutions with increasing concentration of CA 15–3 (from 0.010 and 1000 U mL^{-1}, in 10 mmol L^{-1} acetate buffer, pH 4.0) for 30 min, followed by electrochemical measurements in the presence of the biocompatible reporting system. SWV was selected as electroanalytical technique to quantify CA 15–3 biomarker due to its high sensitivity to surface-confined electrode reactions and fast data acquisition (few seconds only) [36,37].

The voltammograms obtained for the several standard solutions tested are represented in Fig. 4. A decrease of the redox probe peak current with increasing CA 15–3 concentration was observed due to the cumulative immunecomplex formation at the sensor surface which increasingly hinders the redox probe diffusional behavior. Moreover, the SWV peak current was represented as a function of the logarithm of CA 15–3 concentration, as shown in the inset of Fig. 4, and a linear pattern was observed for concentrations between 1.0 and 1000 U mL^{-1}. A limit of detection (LOD) of 0.95 U mL^{-1} was estimated according to the IUPAC recommendations for ion-selective electrodes, where log(C) is used [38]. Thus, the developed immunosensor had a wide range of linearity, allowing direct analysis of CA 15–3 breast cancer biomarker above and below its cut-off value (30 U mL^{-1} [3]).

The analytical features of the developed immunosensor was also compared with other detection approaches reported in the literature (see Table S2, SI). The detection levels (LOD) achieved by the developed immunosensor was of the same order of magnitude of most of reported methodologies, including commercially available ELISA tests, while it had the widest dynamic linear concentration working range for CA 15–3 detection. Nonetheless, it is important to remark that most of these techniques are not label-free (as for the biosensor of this work) since they make use of either secondary antibodies and/or metal/magnetic NPs or nanocomposites, to push sensitivity up and reduce, in turn, detection limit. For example, although FRET immunosensing [39] allowed the ultrasensitive detection of CA 15–3 (LOD of 0.9 μU mL^{-1}), antibody-functionalized carbon dots were used as donor fluorescence and AuNPs labeled PAMAM-Dendrimer/aptamer were used as quencher. In another work, an electrochemical biosensor was developed for the highly sensitive detection of CA 15–3 (LLOQ of 15 μU mL^{-1}) in plasma, however, streptavidin-coated magnetic beads conjugated with biotinylated HRP and biotinylated mAb were used as signal enhancer [40]. Thus, those complex amplification strategies have some limitations associated, such as laborious and time-consuming procedures, need of expensive chemical labels, steric hindrance, among others. By opposition, the developed immunosensor offers simplicity of construction and of use and cost-effective and label-free detection, which are important advantages over other sensors described in the literature. Still, similar LOD (of 0.3 U mL^{-1}) to the obtained in this work was reported in the literature for the label-free electrochemical detection of CA 15–3 based on the catalytic activity of a CuS/rGO nanocomposite [41]. Furthermore, the use of low cost and disposable chips, the AuSPEs, was another crucial aspect in this work since its combination with simple and compact instrumentation allowed the detection of CA 15–3 cancer biomarker in PoC.

Accuracy and reproducibility of the immunosensor was evaluated by repetitive measurements performed to build calibration curves, obtained under the same experimental conditions on different days. The mean relative standard deviation (RSD) value for solutions tested was only 2.8%, indicating that chip surface modification and biosensor response was reproducible. Furthermore, low RDS values (<4%) were reported by our research group [42] for repetitive probe measurements at the bare AuSPE surface, reinforcing that reliable electrochemical immunosensors can be build using ferricyanide/ferrocyanide redox probe as reporting system.

3.4. Selectivity study

The quantification of the target biomarker was also performed in the presence of potential biological interferents which may be present in real serum samples, such as CA 125 or CA 19–9 [43]. In this work, the selectivity of the antibody to its antigen was evaluated by recording the SPR response (see Fig. S4, SI) for detecting 30 U mL^{-1} CA 15–3 in the absence and presence of CA 125 (C = 15 U mL^{-1}) and CA 19–9 (C = 25 U mL^{-1}), as shown in Fig. 5. As can be seen, the sensor response to pure interferent solution was very similar to the response obtained for the blank solution. Moreover, the SPR angle variation due to CA 15–3 solution was very similar to the recorded for the mixture (CA 15–3 + CA

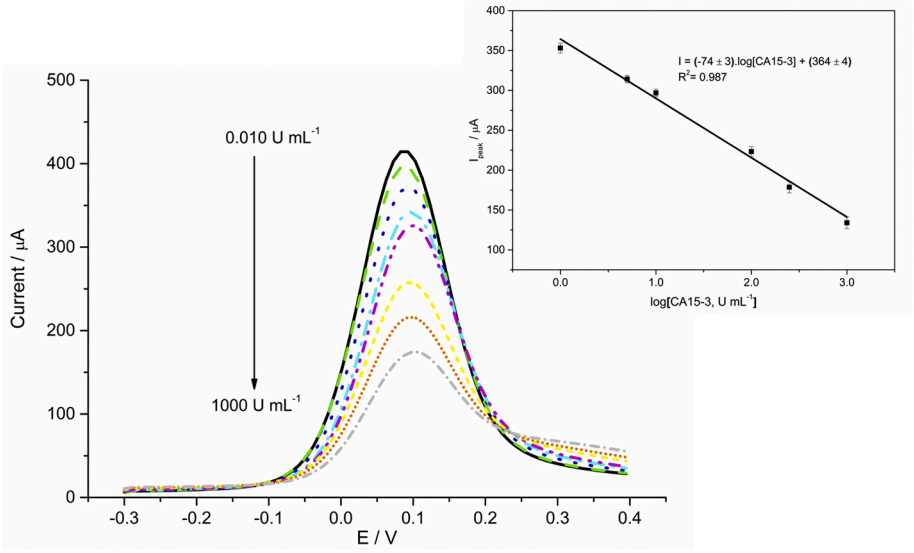

Fig. 4. SWV measurements, recorded in presence of 5 mmol L^{-1} $[Fe(CN)_6]^{3-/4-}$ redox couple, prepared in 0.1 mol L^{-1} Na_2SO_4 electrolyte solution, after incubation of the sensor surface with solutions with increasing concentration of CA 15–3 (from 0.010 to 1000 U mL^{-1}) for 30 min. Inset: Calibration curve obtained for CA 15–3 biomarker by using mean value ± standard deviation ($n \geq 3$).

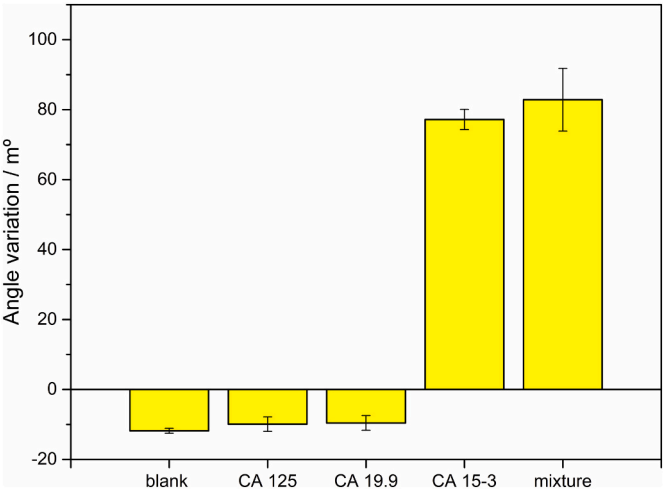

Fig. 5. Selectivity of the developed immunsensor evaluated by recording the SPR angle change after injection on the measuring channel of (i) buffer solution (without CA 15–3 or interferent; blank), (ii) buffer solutions containing (I) 15 U mL^{-1} of CA 125, (II) 25 U mL^{-1} of CA 19–9 and (III) 30 U mL^{-1} of CA 15–3 and a (iii) mixture solution composed of 30 U mL^{-1} CA 15–3, 15 U mL^{-1} CA 125 and 25 U mL^{-1} CA 19–9. Error bars indicate the standard deviation of the optical signal obtained from triplicate measurements (three independent immunoassays for each solution).

125 + CA 19–9; angle variation was only 7.3%), indicating that the immobilized polyclonal antibody was highly selective to the CA 15–3 marker.

It is important to notice that the selectivity of the biosensor was ensured by the antibody specific response to the analyte during the incubation step. Thus, possible interferences to the electrochemical detection, such as ascorbic acid and other electroactive biomolecules that might be present in blood samples, will be wash out from the sensor surface before the electrochemical measurements and no interference from electroactive species was expected.

3.5. Application to CA 15–3 detection in serum

In this work, detection of CA 15-3 in (artificial) serum samples was also performed. The developed immunosensor was not applied to real samples due to ethical issues and regulatory aspects regarding authorizations that make it difficult to obtain and apply real samples in the laboratory context. Thus, artificial serum with a similar composition of the serum from biological samples [28] was used in the experiments. The samples were diluted (1:20, in 10 mmol L^{-1} acetate buffer, pH 4.0) prior the measurements to minimize matrix effects.

Data obtained from electrochemical experiments allowed to build the assay calibration curve (see Fig. S5, SI). Then, the estimated analytical features of the immunosensor in serum were compared with the obtained in buffer solution in terms of detection sensitivity, LODs achieved, linear concentration ranges, etc. (see Table S3, SI). Although the results showed a decrease of detection sensitivity (of about 29%) relatively to buffer solution, probably due to non-specific binding of serum proteins to the sensor surface, the immunosensor kept the same linear concentration range (1.0–1000 U mL^{-1}) and similar LODs were archived, indicating that the developed immunosensor was suitable for quantification of the CA 15–3 biomarker in the prepared serum samples.

The applicability of the proposed sensor was assessed by the recovery study. To perform these studies, blank artificial serum samples were spiked with known amounts of CA 15–3 (from 0.30 to 50 U mL^{-1}) for evaluation of the immunosensor response. The results obtained for three samples in triplicate with different concentration levels are summarized in Table 1. The results showed that there was a good relationship between added and found amounts of CA 15–3 and detection recoveries between 93.3% and 106.8% were achieved (average relative error of 5.4%). Thus, in our opinion, the improved performance of the developed immunosensor indicates that it can be successfully applied for the detection of CA 15–3 in real biofluids in clinical setting.

Table 1
Determination of CA 15–3 in artificial serum.

Sample	CA 15–3 (U mL^{-1})	Found (U mL^{-1})	Recovery (%)	Relative error (%)
1	3.0	3.2 ± 0.5	107 ± 7	−6.7
2	30	30 ± 3	99 ± 8	1.3
3	50	53 ± 6	107 ± 5	−6.8

4. Conclusions

In this work, we have developed and optimized an amperometric immunosensor for simple and rapid screening of CA 15–3 biomarker, in PoC, being a valuable resource under clinical setting for the early diagnosis of breast cancer disease. Low-cost and disposable chips, the AuSPEs, were used to build the electrochemical device since it combines properties of good biocompatibility, ease of use, portability (compatible with PoC testing) and low sample volume for detection.

The biosensing platforms were prepared by simple and efficient immobilization of CA 15–3 antibody over a pre-formed MSA SAM. They were able to detect and quantify the tumor marker by performing electrochemical measurements upon cumulative immunecomplex formation at the sensor surface, which continuously hinders the diffusional redox probe behavior at the electrode surface.

The developed immunosensor presented improved performance and good analytical features were achieved, namely: (i) wide dynamic concentration linear range (from 1.0 to 1000 U mL^{-1}) for easy detection of CA 15–3 levels below and above its cut-off value; (ii) good selectivity towards CA 15–3, allowing its detection in the presence of co-existing cancer biomarkers (CA 125 and CA 19–9) in serum samples; (iii) low detections levels were achieved (LOD of 0.60 U mL^{-1}), allowing the quantification of the biomarker in (artificial) serum at clinically relevant levels.

In our opinion, the high sensitivity (and selectivity) of the developed electrochemical device makes it suitable to be applied to the analysis of CA 15–3 in real serum samples, in clinical context. Besides, the label-free, simple and cost-effective detection has unique advantages over classical immunosensors, most of times having tedious and complex procedures and/or requiring expensive tags (secondary antibodies, conjugated or not with NPs or other nanomaterials, etc.) for signal amplification.

Declaration of Competing Interest

The authors declare no conflict of interest.

Acknowledgements

This research had the financial support of FCT (Fundação para a Ciência e Tecnologia) and co-financed by the European Union (FEDER funds) under the Partnership Agreement PT2020, Research Grants Pest-C/QUI/UIDB/00081/2020 (CIQUP) and NORTE-01-0247-FEDER-017834 (project RamSERS). J.A. Ribeiro (ref. SFRH/BPD/105395/2014) and C.M. Pereira (ref. SFRH/BSAB/150320/2019) acknowledge FCT under the QREN – POPH – Advanced Training, subsidized by European Union and national MEC funds.

Appendix A. Supplementary data

Supplementary data to this article can be found online at https://doi.org/10.1016/j.sbsr.2021.100445.

References

[1] W.-W.H. Organization, Cancer Country Profiles, 2018 (Accessed 30 the september 2019).

[2] J.G. Geraghty, E.C. Coveney, F. Sherry, N.J. Ohiggins, M.J. Duffy, C-15-3 in patients with locoregional and metastatic breast-carcinoma, Cancer 70 (12) (1992) 2831–2834.

[3] S. Chourin, D. Georgescu, C. Gray, C. Guillemet, A. Loeb, C. Veyret, J.P. Basuyau, Value of CA 15-3 determination in the initial management of breast cancer patients, Ann. Oncol. 20 (5) (2009) 962–964.

[4] M.J. Duffy, D. Evoy, E.W. McDermott, CA 15-3: uses and limitation as a biomarker for breast cancer, Clin. Chim. Acta 411 (23–24) (2010) 1869–1874.

[5] R.M. Gonzalez, S.L. Seurynck-Servoss, S.A. Crowley, M. Brown, G.S. Omenn, D. F. Hayes, R.C. Zangar, Development and validation of sandwich ELISA microarrays with minimal assay interference, J. Proteome Res. 7 (6) (2008) 2406–2414.

[6] A. Ambrosi, F. Airo, A. Merkoci, Enhanced gold nanoparticle based ELISA for a breast Cancer biomarker, Anal. Chem. 82 (3) (2010) 1151–1156.

[7] P.H. Li, H.M. Ye, J.W. Liu, H.W. Jin, Y.Z. Lin, S.D. Yan, Y. Yu, L. Gao, F.H. Xu, Z. Y. Zhang, Evaluation of a newly developed quantitative determination kit for tumor marker CA15-3 with chemiluminescent assay, J. Clin. Lab. Anal. 32 (1) (2018).

[8] Z. Fu, Z. Yang, J. Tang, H. Liu, F. Yan, H. Ju, Channel and substrate zone two-dimensional resolution for chemiluminescent multiplex immunoassay, Anal. Chem. 79 (19) (2007) 7376–7382.

[9] B. Babamiri, R. Hallaj, A. Salimi, Ultrasensitive electrochemiluminescence immunoassay for simultaneous determination of CA125 and CA15-3 tumor markers based on PAMAM-sulfanilic acid-Ru(bpy)(3)(2+) and PAMAM-CdTe@CdS nanocomposite, Biosens. Bioelectron. 99 (2018) 353–360.

[10] X.Y. Jiang, H.J. Wang, R. Yuan, Y.Q. Chai, Sensitive electrochemiluminescence detection for CA15-3 based on immobilizing luminol on dendrimer functionalized ZnO nanorods, Biosens. Bioelectron. 63 (2015) 33–38.

[11] I.A. Darwish, T.A. Wani, N.Y. Khalil, D.A. Blake, Novel automated flow-based immunosensor for real-time measurement of the breast cancer biomarker CA15-3 in serum, Talanta 97 (2012) 499–504.

[12] Y.M. Park, S.J. Kim, K. Kim, Y.D. Han, S.S. Yang, H.C. Yoon, Lectin-based optical sensing for quantitative analysis of cancer antigen CA15-3 as a breast cancer marker, Sensors Actuat. B-Chem. 186 (2013) 571–579.

[13] M. Li, J.W. Kang, S. Sukumar, R.R. Dasari, I. Barman, Multiplexed detection of serological cancer markers with plasmon-enhanced Raman spectro-immunoassay, Chem. Sci. 6 (7) (2015) 3906–3914.

[14] W.S. Wang, S. Li, G.N. Zhang, J.X. He, Z.Q. Ma, Electrochemical immunoassay for breast cancer markers CA153 determination based on carbon nanotubes modified electrode, Int. J. Electrochem. Sci. 12 (11) (2017) 10791–10799.

[15] M.S. Wilson, W.Y. Nie, Multiplex measurement of seven tumor markers using an electrochemical protein chip, Anal. Chem. 78 (18) (2006) 6476–6483.

[16] D.P. Tang, R. Yuan, Y.Q. Chai, Biochemical and immunochemical characterization of the antigen-antibody reaction on a non-toxic biomimetic interface immobilized red blood cells of crucian carp and gold nanoparticles, Biosens. Bioelectron. 22 (6) (2007) 1116–1120.

[17] J. Wu, Y.T. Yan, F. Yan, H.X. Ju, Electric field-driven strategy for multiplexed detection of protein biomarkers using a disposable reagentless electrochemical immunosensor array, Anal. Chem. 80 (15) (2008) 6072–6077.

[18] J. Wu, F. Yan, X.Q. Zhang, Y.T. Yan, J.H. Tang, H.X. Ju, Disposable reagentless electrochemical immunosensor array based on a biopolymer/sol-gel membrane for simultaneous measurement of several tumor markers, Clin. Chem. 54 (9) (2008) 1481–1488.

[19] B.Q. Liu, Q.F. Li, B. Zhang, Y.L. Cui, H.F. Chen, G.N. Chen, D.P. Tang, Synthesis of patterned nanogold and mesoporous CoFe2O4 nanoparticle assemblies and their application in clinical immunoassays, Nanoscale 3 (5) (2011) 2220–2226.

[20] G.J. Wang, Y. Qing, J.L. Shan, F. Jin, R. Yuan, D. Wang, Cation-exchange antibody labeling for simultaneous electrochemical detection of tumor markers CA15-3 and CA19-9, Microchim. Acta 180 (7–8) (2013) 651–657.

[21] T. Sawaguchi, Y. Sato, F. Mizutani, Ordered structures of self-assembled monolayers of 3-mercaptopropionoc acid on au(111): *in situ* scanning tunneling microscopy study, Phys. Chem. Chem. Phys. 3 (2001) 3399–3404.

[22] S.S.F.T.C. Moreira, R.A.F. Dutra, J.P.C. Noronha, A.E.G. Cass, M.G.F. Sales, Smart plastic antibody material (SPAM) tailored on disposable screen printed electrodes for protein recognition: application to myoglobin detection, Biosens. Bioelectron. 45 (2013) 237–244.

[23] F. Luderer, U. Walschus, Immobilization of oligonucleotides for biochemical sensing by self-assembled monolayers: thiol-organic bonding on gold and silanization on silica surfaces, Materials 260 (2005) 37–56.

[24] M. Braiek, B.K. Rokbani, A. Chrouda, B. Mrabet, A. Bakhrouf, A. Maaref, N. Jaffrezic-Renault, An electrochemical Immunosensor for detection of Staphylococcus aureus Bacteria based on immobilization of antibodies on self-assembled Monolayers-functionalized gold electrode, Biosensors 2 (4) (2012).

[25] K.P.G. Ralloff, P. Westh, R.A. Purssell, M. Pudek, Y. Koga, Non-ideality of methanol solution's of artificial serum in the mole fraction range from 5 x 10(−4) to 5 x 10 (−3) at 25 degrees C, Fluid Phase Equilib. 207 (1–2) (2003) 301–317.

[26] S. Berchmans, R.G. Nirmal, G. Prabaharan, A.K. Mishra, V. Yegnaraman, Solution phase electron transfer versus bridge mediated electron transfer across carboxylic acid terminated thiols, J. Solid State Electrochem. 10 (7) (2006) 439–446.

[27] A. Krolikowska, J. Bukowska, Self-assembled monolayers of mercaptosuccinic acid on silver and gold surfaces designed for protein binding. Part I: structure of the monolayer, J. Raman Spectrosc. 38 (7) (2007) 936–942.

[28] Z. Pei, H. Anderson, A. Myrskog, G. Dunér, B. Ingemarsson, T. Aastrup, Optimizing immobilization on two-dimensional carboxyl surface: pH dependence of antibody orientation and antigen binding capacity, Anal. Biochem. 398 (2) (2010) 161–168.

[29] S. Löfås, A. McWhirter, The art of immobilization for SPR sensors, in: J. Homola (Ed.), Surface Plasmon Resonance Based Sensors, Springer Berlin Heidelberg, Berlin, Heidelberg, 2006, pp. 117–151.

[30] S. Löfås, B. Johnsson, Å. Edström, A. Hansson, G. Lindquist, R.-M.M. Hillgren, L. Stigh, Methods for site controlled coupling to carboxymethyldextran surfaces in surface plasmon resonance sensors, Biosens. Bioelectron. 10 (9) (1995) 813–822.

[31] J. Buijs, D.D. White, W. Norde, The effect of adsorption on the antigen binding by IgG and its F(ab')2 fragments, Colloids Surf. B: Biointerfaces 8 (4) (1997) 239–249.

[32] S.G. Patching, Surface plasmon resonance spectroscopy for characterisation of membrane protein-ligand interactions and its potential for drug discovery, Biochim. Biophys. Acta-Biomembr. 1838 (1) (2014) 43–55.

[33] J. Homola, Surface Plasmon resonance sensors for detection of chemical and biological species, Chem. Rev. 108 (2) (2008) 462–493.

[34] H. Dong, X.D. Cao, C.M. Li, W.H. Hu, An in situ electrochemical surface plasmon resonance immunosensor with polypyrrole propylic acid film: comparison between SPR and electrochemical responses from polymer formation to protein immunosensing, Biosens. Bioelectron. 23 (7) (2008) 1055–1062.

[35] J. Wu, Y. Yan, F. Yan, H. Ju, Electric field-driven strategy for multiplexed detection of protein biomarkers using a disposable reagentless electrochemical immunosensor array, Anal. Chem. 80 (15) (2008) 6072–6077.

[36] E.K. Wujcik, H. Wei, X. Zhang, J. Guo, X. Yan, N. Sutrave, S. Wei, Z. Guo, Antibody nanosensors: a detailed review, RSC Adv. 4 (82) (2014) 43725–43745.

[37] F. Ricci, G. Adornetto, G. Palleschi, A review of experimental aspects of electrochemical immunosensors, Electrochim. Acta 84 (2012) 74–83.

[38] R.P. Buck, E. Lindner, Recommendations for nomenclature of ion-selective electrodes (IUPAC recommendations 1994), Pure Appl. Chem. 66 (12) (1994) 2527–2536.

[39] S. Mohammadi, A. Salimi, S. Hamd-Ghadareh, F. Fathi, F. Soleimani, A FRET immunosensor for sensitive detection of CA 15-3 tumor marker in human serum sample and breast cancer cells using antibody functionalized luminescent carbon-dots and AuNPs-dendrimer aptamer as donor-acceptor pair, Anal. Biochem. 557 (2018) 18–26.

[40] S. Akbari Nakhjavani, B. Khalilzadeh, P. Samadi Pakchin, R. Saber, M. H. Ghahremani, Y. Omidi, A highly sensitive and reliable detection of CA15-3 in patient plasma with electrochemical biosensor labeled with magnetic beads, Biosens. Bioelectron. 122 (2018) 8–15.

[41] J. Amani, A. Khoshroo, M. Rahimi-Nasrabadi, Electrochemical immunosensor for the breast cancer marker CA 15-3 based on the catalytic activity of a CuS/reduced graphene oxide nanocomposite towards the electrooxidation of catechol, Microchim. Acta 185 (1) (2018).

[42] J.A. Ribeiro, E. Silva, P.S. Moreira, C.M. Pereira, Electrochemical characterization of redox probes at gold screen-printed electrodes: efforts towards signal stability, ChemistrySelect 5 (17) (2020) 5041–5048.

[43] U.K. Ballehaninna, R.S. Chamberlain, The clinical utility of serum CA 19–9 in the diagnosis, prognosis and management of pancreatic adenocarcinoma: An evidence based appraisal, J. Gastrointest. Oncol. 3 (2 (June 2012)) (2011).